INFLUENCE OF GROWTH CONDITIONS ON STRUCTURAL AND OPTICAL PROPERTIES OF $Zn_{0.9}Cd_{0.1}O$ FILMS

I.I. SHTEPLIUK,[1] G.V. LASHKAREV,[1] V.V. KHOMYAK,[2] O.S. LYTVYN,[3] P.D. MARIANCHUK,[2] I.I. TIMOFEEVA,[1] A.I. EVTUSHENKO,[1] V.I. LAZORENKO[1]

[1]**Institute for Problems of Materials Science, Nat. Acad. of Sci. of Ukraine**
(3, Krzhyzhanivskyi Str., Kyiv 03142, Ukraine; e-mail: shtepliuk_1987@ukr.net)

[2]**Yu. Fedkovych Chernivitsi National University**
(2, Kotsyubynskyi Str., Chernivtsi 58012, Ukraine)

[3]**V. Lashkaryov Institute of Semiconductor Physics, Nat. Acad. of Sci. of Ukraine**
(45, Prosp. Nauky, Kyiv 03028, Ukraine)

The influence of the magnetron power and the gas ratio Ar:O_2 on the microstructure and the optical properties of $Zn_{0.9}Cd_{0.1}O$ films is studied. The films were deposited with the use of the dc magnetron sputtering technique at a temperature of 250 °C. Atomic force microscopy (AFM) and X-ray diffraction (XRD) researches of a surface morphology demonstrated a strong influence of deposition procedure parameters on the film microstructure. The XRD analysis revealed that all grown films were polycrystalline and single-phase. The increase of the gas ratio Ar:O_2 was found to be beneficial for the crystalline structure of $Zn_{0.9}Cd_{0.1}O$ ternary alloys. Peculiarities of the control over the band gap and the surface morphology for $Zn_{0.9}Cd_{0.1}O$ ternary alloys by varying the growth parameters are discussed.

1. Introduction

Semiconductor materials on the basis of ZnO are considered as the most promising ones for the creation of highly effective light-emitting and laser diodes, which operate in the ultra-violet and visible spectral ranges. This circumstance is connected with the direct-bandgap structure of the electron spectrum (3.37 eV) and a large binding energy of excitons (60 meV) in zinc oxide [1–3]. An important factor at the development of optoelectronic devices – especially, light-emitting and laser diodes with a high emittance – is the ability to control the energy gap, which is necessary for the formation of quantum wells [4–6]. A reduction of the energy gap width in zinc oxide can be realized by creating the solid solutions ZnO + CdO. In the previous works [7–16], the films of solid solutions $Zn_{1-x}Cd_xO$ were mainly grown up, by using molecular beam epitaxy and the deposition from the gas phase taking advantage of metal-organic compounds. Despite that considerable efforts were made by various scientific groups, the optical efficiency of $Zn_{1-x}Cd_xO$ films remains still unsatisfactory. This fact is undoubtedly connected with restrictions of the physical origin, which counteract the growing of structurally perfect $Zn_{1-x}Cd_xO$ films. This circumstance does not allow the multipurpose capabilities of this semiconductor system to be used in optoelectronics at the present stage of researches. It should be noted that the main physical problems at growing $Zn_{1-x}Cd_xO$ layers are associated with a mismatch between the crystal lattices in wurtzite ZnO and cubic CdO, a weak solubility of cadmium in the zinc oxide matrix (2%), and a difference between the ionic radii of Zn and Cd (22%). The indicated factors can promote a non-uniform distribution of cadmium in growing solid solution films and induce a spinodal decay of the system and a phase separation. In order to create highly effective heterostructures with a quantummechanical confinement on the basis of zinc oxide, e.g., $ZnO/Zn_{1-x}Cd_xO/ZnO$, two requirements are compulsory: a modification of the ZnO band spectrum and a high structural perfection of ZnO solid solution films. An increase of the cadmium content in alloy-based targets used for sputtering can provide a modification of the zinc oxide energy spectrum. At the same time, it results in a deterioration of the structural and optical quality of solid solutions, because a significant number of intrinsic defects emerge, and the concentration of dislocations increases. Therefore, there arises the problem connected with the search for an alternative way to control the microstructure parameters and the energy gap width, which would exclude the application of targets with an elevated cadmium content in the magnetron sputtering process.

In this work, we used the dc magnetron sputtering technique, which allows high-quality ZnCdO films on sapphire substrates to be grown up. Magnetron sputtering is characterized by such advantages as relatively low temperatures of a substrate, the good film adhesion, the good uniformity across the film thickness, a high film density, and a capability of the direct deposition from metal targets by the reactive sputtering in gas mixtures [17]. Since the ratio of working gases and the magnetron power are critical parameters for this deposition method, a research of their influence on microstructural and optical properties of solid solution films is a challenging physical problem from the viewpoint of both materials science and technology.

This work is aimed at the determination of regularities in the formation of solid solutions depending on parameters of the magnetron sputtering process and at the study of capabilities to control the energy spectrum and structural properties of $Zn_{0.9}Cd_{0.1}O$ semiconductor films by varying the ratio between the partial pressures of working gases and the magnetron power. In addition, physical mechanisms of the influence of technological parameters on the fundamental characteristics of the solid solution under study are proposed.

2. Experimental Part

$Zn_{1-x}Cd_xO$ films ($x = 0.10$) were grown up using the method of dc magnetron sputtering on sapphire substrates (c-Al_2O_3) at a temperature of 250 °C. As targets for sputtering, we used disks fabricated of zinc and cadmium alloy (100 mm in diameter and a purity degree of 99.99%). High-purity argon and oxygen were used as working gases. The distance between the target and the substrate was 40 mm. The residual pressure in the deposition chamber was 1×10^{-4} Pa. To study the influence of working gases on the properties of deposited films, we varied the ratio $Ar:O_2$ from 2:1 to 4:1. The time of the permanent sputtering was 1 h. The magnetron power was varied within the limits from 100 to 150 W.

The surface morphology (grain dimension and surface roughness) was studied with the help of an atomic-power microscope (AFM) Nanoscope III (Digital Co. Instruments, USA) and with the use of a silicon probe. The surface was scanned in the tapping mode. All measurements were carried out at room temperature. In our researches, the surface roughness RMS was determined as follows: $RMS = [\Sigma(z_i - z_{av})^2/N]^{1/2}$, where z_i is a current z-value, z_{av} is the z-value averaged over the scanned region, and N is the number of points. The

grain sizes were evaluated with the help of the Cross Section Analysis Nano-Scope III software program.

The crystalline structure of specimens was studied using the X-ray diffraction (XRD) technique. CuK_{α} radiation ($\lambda = 0.154056$ nm) was used as a source. XRD measurements were carried out on a DRON-4 diffractometer. Scanning electron microscopy (SEM) was used to estimate the uniformity of deposited films and the quality of the film/substrate interface. The element analysis of ZnCdO films was executed using the method of X-ray spectral microanalysis on a ZEISS EVO 50 XVP scanning electron microscope with the help of an energy dispersive spectrometer equipped with an INCA450 system (Oxford Instruments). The optical transmittance of films was measured on an SF-2000 spectrophotometer at room temperature.

3. Results and Their Discussion

The XRD data obtained brought us to the conclusion that all specimens were polycrystalline and single-phase. They crystallized into a hexagonal structure of the "wurtzite" type, with the overwhelming number of crystallites being orientated along the c-axis. It should be noted that we did not reveal any diffraction peaks that would correspond to CdO or other phases. The Bragg angle for the main peak, which corresponded to the (002) crystallographic plane, was equal to 34.05° and 34.12° for $Zn_{0.9}Cd_{0.1}O$ films grown up at the magnetron power $P = 100$ W and the ratios between the pressures of working gases of 2:1 and 4:1, respectively. The growth of the magnetron power to 150 W was accompanied by a decrease of the Bragg angle to 33.99 and 33.96°, respectively. The lattice periods a and c were calculated according to the following relations [18]:

$$c = \frac{\lambda}{\sin\theta}; \quad a = \sqrt{\frac{1}{3}}\frac{\lambda}{\sin\theta}.$$

The growth of the lattice periods together with the growth of the magnetron power from 100 to 150 W (see Table 1) indicates that $Zn_{0.9}Cd_{0.1}O$ films are in a uniformly stressed state, with the stretching component being oriented in parallel with the c-axis. The reason for this variation of the lattice parameters consists in that more cadmium ions entered into the cation sublattice of ZnO at a higher magnetron power. The calculation of stresses in the film was based on the biaxial strain model. The strain $\varepsilon = (c_{film} - c_{bulk})/c_{bulk}$ along the c-axis, i.e. normally to the substrate surface, was determined from the XRD data ($c_{bulk} = 5.2054$ Å). To calculate the total strain magnitude at a given growth temperature, i.e.

T a b l e 1. Microstructure parameters calculated on the basis of XRD analysis

Specimen	Ratio of working gas pressures Ar:O_2	Magnetron power P, W	Diffraction angle $2\theta_{002}$, deg.	Half-width, deg.	Lattice period a, Å	Lattice period c, Å	CSR size D, nm	Dislocation concentration $\delta \times 10^{15}$, m^{-2},	Stresses σ_{film}, GPa,
$Zn_{0.9}Cd_{0.1}O$	2:1	100	34.05	0.965	3.036	5.263	9	12.3	−2.68
$Zn_{0.9}Cd_{0.1}O$	4:1	100	34.12	0.551	3.029	5.250	15	4.4	−2.10
$Zn_{0.9}Cd_{0.1}O$	2:1	150	33.99	1.103	3.040	5.270	7	20.4	−2.99
$Zn_{0.9}Cd_{0.1}O$	4:1	150	33.96	0.525	3.043	5.275	16	3.9	−3.21

$\varepsilon(T_{\text{sub}})$, it is necessary that, besides the residual microstrain ε, the thermoelastic strain ε_T, which emerges as a result of the difference between the coefficients of thermal expansion for $Zn_{0.9}Cd_{0.1}O$ and Al_2O_3, should also be taken into account. In the calculations, we used the following values for the thermal expansion coefficients: for $Zn_{0.9}Cd_{0.1}O$, $\alpha_{\text{ZnCdO}} \approx \alpha_{\text{ZnO}} = 6.5 \times 10^{-6}$ K^{-1}; and for sapphire, $\alpha_{\text{sapph}} = 4.5 \times 10^{-6}$ K^{-1} [20]. The thermoelastic strain was determined by the formula

$$\varepsilon_T = (\alpha_{\text{ZnO}} - \alpha_{\text{sapph}})\Delta T,$$

where ΔT is the difference between the growth and room temperatures. Then, the total strain is $\varepsilon(T_{\text{sub}}) = \varepsilon + \varepsilon_T$.

To determine the stress σ_{film} in the film, the following formula can be used, which is valid for a hexagonal lattice:

$$\sigma_{\text{film}} = \frac{2c_{13}^2 - c_{33}(c_{11} + c_{12})}{2c_{13}} \varepsilon(T_{\text{sub}}).$$

For the elastic stiffness constants c_{ij} of a ZnO single crystal, the following values were used: $c_{11} = 208.8$ GPa, $c_{33} = 213.8$ GPa, $c_{12} = 119.7$ GPa, and $c_{13} = 104.2$ GPa [21]. Then we arrive at the following relation for the stress: $\sigma_{\text{film}} = -233\varepsilon(T_{\text{sub}})$. For $Zn_{0.9}Cd_{0.1}O$ films, tensile stresses are observed, and the increase in magnetron power leads to a growth of tensile stresses in the films.

The values of diffraction maximum half-width for the (002) crystallographic plane are quoted in Table 1. If the partial pressure of argon increases, the reflex half-width decreases, which testifies to a better structural perfection of films. The dimension of coherent scattering regions (CSRs) D was calculated using the Debye–Scherrer formula [22],

$$D = \frac{0.94\lambda}{\beta \cos\theta}.$$

The dislocation concentration δ, which corresponds to the number of defects in the film, was determined by the formula $d = 1/D^2$ [23]. The values calculated for those quantities are also presented in Table 1. Larger dimensions of crystallites and smaller values of half-width testify to a better crystalline structure of the films.

It should be noted that, for $Zn_{0.9}Cd_{0.1}O$ films, when the magnetron power increased from 100 to 150 W, the lattice period and the tensile stress also grew. Three probable factors are known, which can promote a deterioration in the structural ordering, when the magnetron power increases [24]. First, the deposition rate linearly grows with the capacity. This means that as-sputtered ions of metallic zinc and cadmium have less time to occupy stable equilibrium positions. Second, the power increase may be accompanied by a growth in the relative number of atomic zinc and a reduction in the number of ZnO molecules condensed onto the substrate [24]. Aita et al. [25] reported that the additional stage of oxide formation on the substrate results in that the deposited films become more crystal-disordered than in the case where the already formed oxide molecules are condensed. Third, the energy of secondary electrons emitted from the target in the course of sputtering grows with the applied voltage and, hence, the magnetron power. The collision of secondary electrons bombarding the growing film surface results in that they lose their energy, and, therefore, the film is heated up [26, 27]. The extra heating is created by the stress gradient across the film thickness, in such a manner promoting the non-uniform film growth [28]. Moreover, the electron bombardment of the solid surface and the layer of oxygen adsorbed on it can induce the oxygen desorption [29–31]. This effect can reduce the probability of the stoichiometric oxide formation on the growth interface before the deposition of the next film layer.

When the working gas ratio Ar:O_2 increases from 2 : 1 to 4 : 1, the half-width of a diffraction reflex diminishes, whereas the linear dimension of coherent scattering regions grows (Table 1). Therefore, the films grown up at the ratio Ar:O_2 = 4:1 turned out structurally more perfect than those grown up at a ratio of 2:1. This improvement of the structural perfection of films can be explained by the interaction between argon ions and the substrate surface. Argon ions can either damage the growing film or raise the surface mobility of adatoms. In the latter case, the increase of the adatom surface mobility can improve the quality of the crystal. This
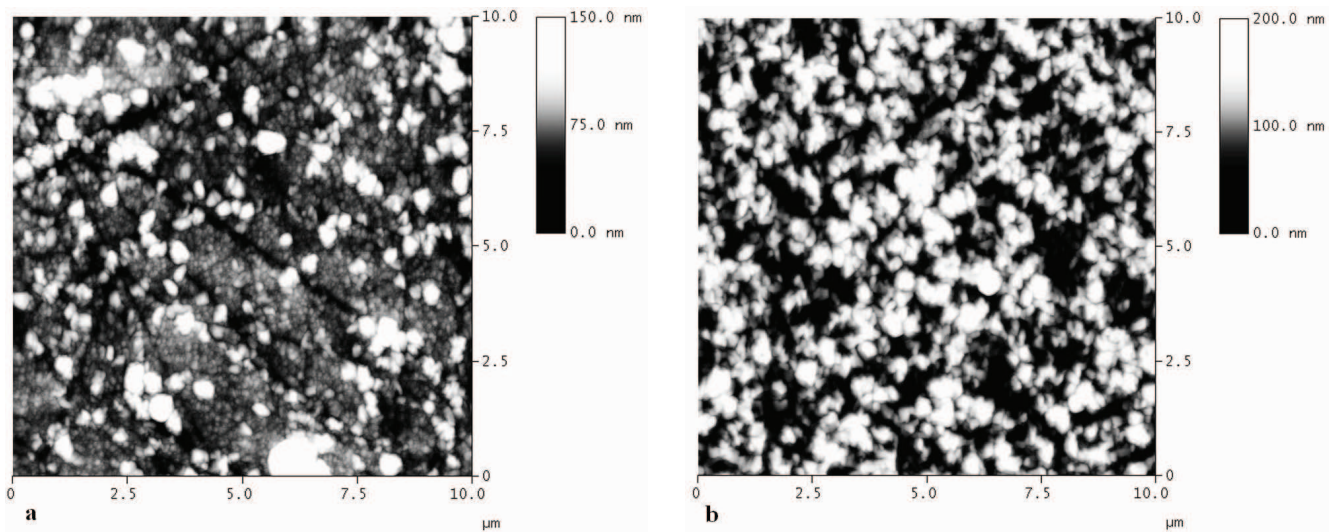
Fig. 1. AFM pictures of $Zn_{0.9}Cd_{0.1}O$ films deposited at a fixed magnetron power of 100 W and various pressure ratios of working gases $Ar:O_2 = 2:1$ (*a*) and 4:1 (*b*)

compromise between the film damage and the beneficial effect of ionic bombardment finds its reflection in two cases presented in this work: $Ar:O_2 = 2:1$ and 4:1. If the content of argon ions in the gas mixture is low (the former case), the sputtered particles move to the substrate and are condensed there at any site that they arrived at. In this case, the processes of surface diffusion and restructuring are restricted, because the interaction between the substrate and the plasma-forming gas can be neglected. In the latter case, the high content of argon ions in plasma not only provides a more intense and more efficient sputtering of the target material, but also gives rise to that high-energy argon ions enhance the surface mobility of adatoms in the course of substrate bombardment. Those circumstances results in that the grain size increases, and the number of intrinsic defects decreases.

The AFM images of the surface of $Zn_{0.9}Cd_{0.1}O$ films grown at various $Ar:O_2$ ratios and a fixed magnetron power P are depicted in Fig. 1. One can see that the surface of the $Zn_{0.9}Cd_{0.1}O$ film grown at $Ar:O_2 = 2:1$ and $P = 100$ W consists of islands 370 nm in diameter and 70 nm in height. The $Zn_{0.9}Cd_{0.1}O$ film deposited at $Ar:O_2 = 4:1$ and $P = 100$ W has an average grain dimension of 530 nm, with the grains being packed more densely. The roughness of the $Zn_{0.9}Cd_{0.1}O$ film surface determined over a 10×10 mm²-fragment was 8 and 32 nm for the films deposited at $Ar:O_2 = 2:1$ and 4:1, respectively.

Hence, if the partial pressure of argon increases, the grain dimensions and the roughness of $Zn_{0.9}Cd_{0.1}O$ films deposited onto sapphire substrates become larger. The influence of the gas ratio $Ar:O_2$ on the surface morphology of $Zn_{0.9}Cd_{0.1}O$ films can be explained by the increase of the number of argon ions in the gas mixture. As a result, the target is sputtered more intensively. The emergence of additional sputtered metal ions of zinc and cadmium induces a considerable acceleration of the film growth rate, which manifests itself as an enlargement of grain dimensions.

An increase of the magnetron power leads to the grain agglomeration, so that the surface becomes rougher (Table 2). This fact can be explained as follows. The power growth enhances the ionization of the reaction gas O_2 and stimulates the appearance of high-energy oxygen ions. Thereof, zinc and cadmium atoms react with atomic oxygen rather than molecular one, which favors the growth rate acceleration and, respectively, the grain enlargement.

The chemical composition of $Zn_{1-x}Cd_xO$ films was determined with the help of X-ray spectral microanalysis. Figure 2 demonstrates a typical energy dispersive

T a b l e 2. **Grain size and surface roughness calculated from the data of AFM analysis**

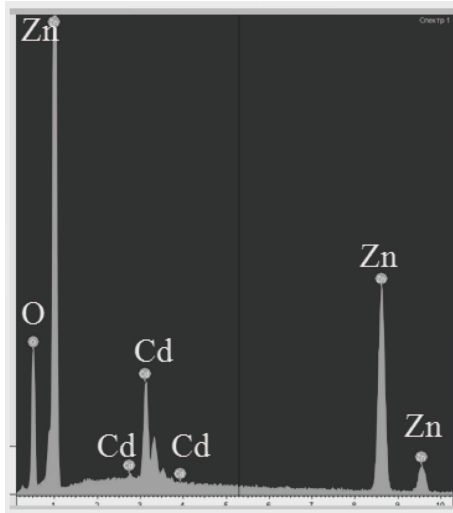| Specimen	Ratio of working gas pressures $Ar:O_2$	Magnetron power P, W	Grain size D_{AFM}, nm	Roughness RMS, nm
$Zn_{0.9}Cd_{0.1}O$	2:1	100	369	8
$Zn_{0.9}Cd_{0.1}O$	4:1	100	531	32
$Zn_{0.9}Cd_{0.1}O$	2:1	150	410	30
$Zn_{0.9}Cd_{0.1}O$	4:1	150	694	39

Fig. 2. Energy dispersive spectrum of a $Zn_{0.9}Cd_{0.1}O$ film grown at a magnetron power of 150 W and the gas ratio $Ar{:}O_2 = 4{:}1$

spectrum of a $Zn_{1-x}Cd_xO$ specimen grown at a magnetron power of 150 W and the gas ratio $Ar{:}O_2 = 4{:}1$. The spectrum confirms the availability of cadmium in the ZnO crystal lattice: the cadmium content is about 13 at.%. At the same time, the cadmium content in the target was 10 at.%. Hence, by varying growth conditions, it is possible to change the cadmium content in the growing films.

In Fig. 3,a, the optical transmittance spectra of $Zn_{0.9}Cd_{0.1}O$ solid solution films grown at various ratios $(Ar{:}O_2)$ of working gas pressures and various magnetron powers are shown. The formation of the solid solution $Zn_{1-x}Cd_xO$ induces a shift of the intrinsic absorption band edge toward the long-wave (low-energy) side of the optical range. Visually, this fact manifests itself in that the initially transparent colorless specimens become dark yellow. On the basis of measured transmittance spectra, the absorption ones were constructed with the use of the relation

$$\alpha = \frac{1}{d}\ln\left[\frac{(1-R)^2}{2T} + \sqrt{\left(\frac{(1-R)^2}{2T}\right)^2 + R^2}\right],$$

where d is the film thickness, R the reflection coefficient ($R = 10\%$), and T the film transmittance. Since $Zn_{0.9}Cd_{0.1}O$ is a direct-gap semiconductor, the spectral dependence of its absorption coefficient α satisfies the relation $\alpha(h\nu) = A(h\nu - E_g)^{1/2}$, where E_g is the optical width of the energy gap, and A is a constant. The dependences of the quantity $(\alpha h\nu)^2$ on $h\nu$ for $Zn_{0.9}Cd_{0.1}O$ films sputtered at various ratios of working gases $Ar{:}O_2$ and various magnetron powers are presented in Fig. 3,b.
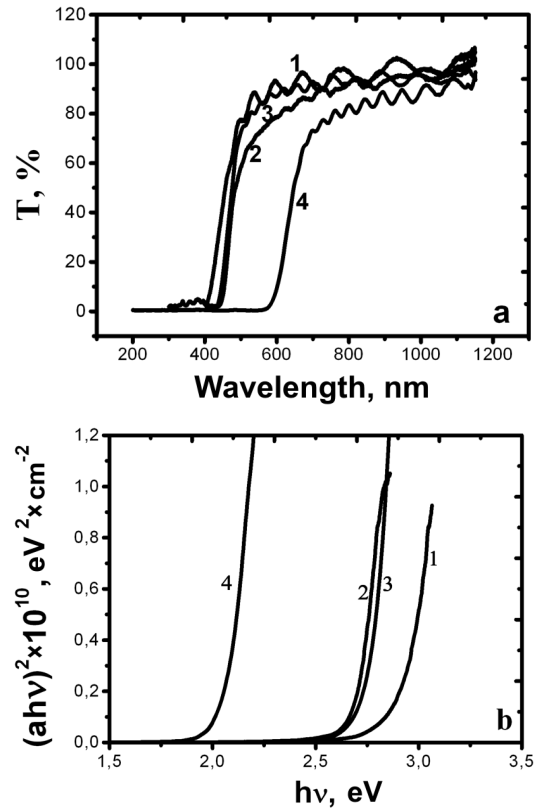

Fig. 3. Optical transmittance spectra (a) and dependences $(\alpha h\nu)^2$ versus $h\nu$ (b) for $Zn_{0.9}Cd_{0.1}O$ films grown at various $Ar{:}O_2$ ratios and magnetron powers: 2:1, 100 W (1); 4:1, 100 W (2); 2:1, 150 W (3); and 4:1, 150 W (4)

The E_g-values can be obtained by extrapolating every curve to $(\alpha h\nu)^2 = 0$.

At the gas ratios $Ar{:}O_2 = 2{:}1$ and 4:1 and at a fixed magnetron power of 100 W, the energy gap width in $Zn_{0.9}Cd_{0.1}O$ is 2.917 and 2.69 eV, respectively. The displacement of the energy gap width into the low-energy spectral range testifies that more cadmium ions substituted zinc ones in the cation sublattice of ZnO in the course of solid solution formation. It is so, because, under such conditions, the majority of cadmium atoms have enough time to be oxidized and to diffuse into the growing film. Accordingly, the energy gap width gradually decreases as the cadmium content in the film increases. Moreover, the influence of the working gas ratio on the optical width of the energy gap in zinc oxide solid solution films can be explained as follows. Conduction electrons in zinc oxide are known to be mainly generated by oxygen vacancies and zinc interstitial atoms. Therefore, the reduction of the energy gap width, when the oxygen pressure decreases, can be connected with the
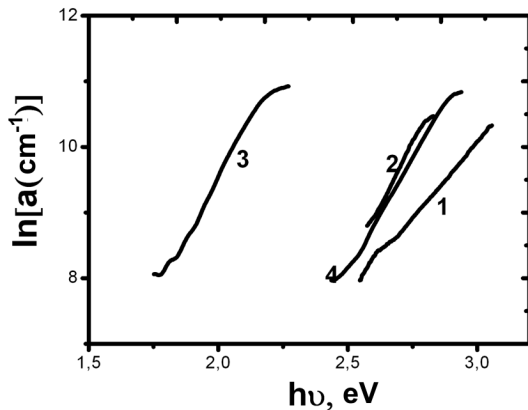
Fig. 4. Dependences $\ln \alpha$ versus $h\upsilon$ for $Zn_{0.9}Cd_{0.1}O$ films grown at various $Ar{:}O_2$ ratios and magnetron powers: 2:1, 100 W (*1*); 4:1, 100 W (*2*); 2:1, 150 W (*3*); and 4:1, 150 W (*4*)

Fig. 5. Dependences of the optical energy gap width in $Zn_{0.9}Cd_{0.1}O$ films on the growth parameters: the working gas ratio and the magnetron power

appearance of allowed energy levels near the conduction band bottom, which are formed by oxygen vacancies and zinc interstitial atoms.

The magnetron power growth leads to a drastic reduction of the film transparency, which is associated with increase in the number of nonoxidized Zn and Cd atoms at the film interface. The increase of the magnetron power from 100 to 150 W at the fixed gas ratio $Ar{:}O_2 = 2{:}1$ also results in a reduction of the energy gap width in $Zn_{0.9}Cd_{0.1}O$ films from 2.917 to 2.74 eV.

Fluctuations in the solid solution composition give rise to the smearing of the absorption band edge for $Zn_{0.9}Cd_{0.1}O$ films in comparison with that for zinc oxide. In the long-wave part of the spectrum, the absorption tail is described by the Urbach exponential law, being associated with the excitation of electron states in disordered film regions. In this case, the absorption in the interval below the fundamental edge (at $h\upsilon < E_g$) can be described by the expression

$$\alpha(E) = \alpha_0 \exp\left(\frac{E - E_0}{E_U}\right),$$

where α_0 is a constant, E_0 the energy gap width, and E_U the Urbach energy (the Urbach tail) [32]. The latter is known to be directly associated with a similar exponential tail in the density of states [33]. The Urbach tail width can serve as an indicator of the disordering in a semiconductor. Figure 4 shows the dependences of $\ln \alpha$ on $h\upsilon$ obtained for $Zn_{0.9}Cd_{0.1}O$ films grown at various gas ratios $Ar{:}O_2$ and various magnetron powers. The character of those dependences, in general, corresponds to optical transitions between occupied states in the valence band tail and empty states at the edge of the conduction band. The E_U-values were calculated from the
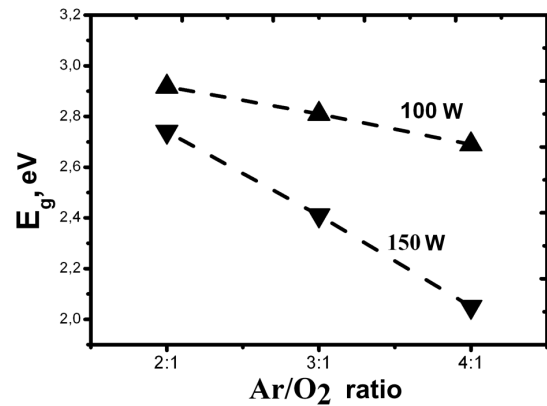
slope of the curves depicted in Fig. 4 using the relation

$$E_U = \left(\frac{d(\ln \alpha)}{d(h\upsilon)}\right)^{-1}.$$

The values of Urbach energy for $Zn_{0.9}Cd_{0.1}O$ films grown at a magnetron power of 100 W are higher than those for films deposited at 150 W. A higher Urbach energy testifies to a higher disorder in solid solutions. If the ratio between working gases $Ar{:}O_2$ increases from 2:1 to 4:1, the Urbach energy for solid solution films decreases from 221 to 137 meV, which is associated with an improvement in the deposited film stoichiometry and a reduction in the number of structural defects. This conclusion correlates with the results of XRD analysis. According to them, the increase of the partial argon pressure in the Ar–O_2 mixture leads to a reduction of the half-width of diffraction peaks (002) and to an expansion of coherence regions. A reduction of the Urbach energy is accompanied by a reduction of the energy gap width in $Zn_{0.9}Cd_{0.1}O$.

The reduction of E_U-value, when the partial argon pressure decreases, can also be connected with modifications in the film microstructure. The atomic power microscopy pattern depicted in Fig. 1 evidences the transformation of the surface with island morphology, which is characteristic of the film grown at the ratio $Ar{:}O_2 = 2{:}1$, into the surface with densely packed grains for a specimen grown at $Ar{:}O_2 = 4{:}1$. The corresponding Urbach energy, the optical width of the energy gap, and the transparency of $Zn_{0.9}Cd_{0.1}O$ films are quoted in Table 3.

In Fig. 5, the dependences of energy gap optical width of $Zn_{0.9}Cd_{0.1}O$ films on the growth parameters – the pressure ratio of working gases and the magnetron power – are shown. The figure makes it evident that there is a capability to control the energy gap width in

T a b l e 3. Optical parameters of $Zn_{0.9}Cd_{0.1}O$ solid solutions grown under various technological conditions

Specimen	Ratio of working gas pressures Ar:O_2	Magnetron power P, W	Urbach energy E_U, meV	Optical width of energy gap E_g, eV	Transmittance T, %
$Zn_{0.9}Cd_{0.1}O$	2:1	100	221	2.917	87
$Zn_{0.9}Cd_{0.1}O$	4:1	100	137	2.69	81
$Zn_{0.9}Cd_{0.1}O$	2:1	150	155	2.74	83
$Zn_{0.9}Cd_{0.1}O$	4:1	150	141	2.05	76

$Zn_{1-x}Cd_xO$ solid solutions by varying the conditions of their deposition. One can see that the change of even a single growth parameters leads to substantial modifications in the energy gap magnitude. This means that, by varying the deposition conditions, it is possible to control the cadmium content in the film and, respectively, the magnitude of E_g.

4. Conclusions

In this work, the influence of technological growth conditions (the magnetron power and the ratio between the partial pressures of working gases) on the microstructure and the energy gap width of $Zn_{0.9}Cd_{0.1}O$ films grown using the method of dc magnetron sputtering is studied. The X-ray duffraction analysis demonstrated that the films obtained were polycrystalline and textured in the crystallographic direction (002). The increase of the working gas ratio Ar:O_2 is found to have a beneficial effect for the crystalline structure of films of $Zn_{0.9}Cd_{0.1}O$ solid solutions. In particular, this fact manifested itself in that the films grown under given conditions were characterized by larger coherent scattering regions, lower dislocation concentrations, and lower Urbach energies. We have found that the microstructure and the energy gap width can be controlled by varying the deposition parameter. Probable mechanisms of the influence of the working gas pressure ratio and the magnetron power on the film growth process are proposed. The results obtained point to a potential way of fabricating the highly texturized films of $Zn_{1-x}Cd_xO$ solid solutions and testify to the capability of a purposeful control over its energy band spectrum and physical parameters making no use of targets with an enhanced cadmium content. Undoubtedly, this can promote the elimination of physical restrictions while growing $Zn_{1-x}Cd_xO$ and allows one to obtain homogeneous semiconductor systems of solid solutions, which are necessary for the development of highly efficient light-emitting devices.

1. A. Tsukazaki, A. Ohtomo, T. Onuma, M. Ohtani, T. Makino, M. Sumiya, K. Ohtani, S.F. Chichibu, S. Fuke, Y. Segawa, H. Ohno, H. Koinuma, and M. Kawasaki, Nature Mater. **4**, 42 (2005).

2. Z.P. Wei, Y.M. Lu, D.Z. Shen, Z.Z. Zhang, B. Yao, B.H. Li, J.Y. Zhang, D.X. Zhao, X.W. Fan, and Z.K. Tang, Appl. Phys. Lett. **90**, 042113 (2007).

3. J.M. Qin, B. Yao, Y. Yan, J.Y. Zhang, X.P. Jia, Z.Z. Zhang, B.H. Li, C.X. Shan, and D.Z. Shen, Appl. Phys. Lett. **95**, 022101 (2009).

4. B.P. Zhang, N.T. Binh, K. Wakatsuki, C.Y. Liu, Y. Segawa, and N. Usami, Appl. Phys. Lett. **86**, 032105 (2005).

5. H.D. Sun, T. Makino, N.T. Tuan, Y. Segawa, Z.K. Tang, G.K.L. Wong, M. Kawasaki, A. Ohtomo, K. Tamura, and H. Koinuma, Appl. Phys. Lett. **77**, 4250 (2000).

6. A. Janotti and C.G.V. De Walle, Rep. Prog. Phys. **72**, 126501 (2009).

7. J.J. Chen, F. Ren, D.P. Norton, S.J. Pearton, A. Osinsky, J.W. Dong, and S.N.G. Chu, Electrochem. Solid-State Lett. **8**, G359 (2005).

8. F.Z. Wang, H.P. He, Z.Z. Ye, and L.P. Zhu, J. Appl. Phys. **98**, 084301 (2005).

9. K. Sakurai, T. Takagi, T. Kubo, D. Kajita, T. Tanabe, H. Takasu, S. Fujita, and S. Fujita, J. Cryst. Growth **514**, 237 (2002).

10. X.J. Wang, I.A. Buyanova, W.M. Chen, M. Izadifard, S. Rawal, D.P. Norton, S.J. Pearton, A. Osinsky, J.W. Dong, and A. Dabiran, Appl. Phys. Lett. **89**, 151909 (2006).

11. J. Zuniga-Perez, V. Munoz-Sanjose, M. Lorenz, G. Benndorf, S. Heitsch, D. Spemann, and M. Grundmann, J. Appl. Phys. **99**, 023514 (2006).

12. J. Ishihara, A. Nakamura, S. Shigemori, T. Aoki, and J. Temmyo, Appl. Phys. Lett. **89**, 091914 (2006).

13. S. Kalusniak, S. Sadofev, J. Puls, and F. Henneberger, Laser Photonics Rev. **3**, 233 (2009).

14. A.V. Thompson, C. Boutwell, J.W. Mares, W.V. Schoenfeld, A. Osinsky, B. Hertog, J.Q. Xie, S.J. Pearton, and D.P. Norton, Appl. Phys. Lett. **91**, 201921 (2007).

15. I.A. Buyanova, X.J. Wang, G. Pozina, W.M. Chen, W. Lim, D.P. Norton, S.J. Pearton, A. Osinsky, J.W. Dong, and B. Hertog, Appl. Phys. Lett. **92**, 261912 (2008).

16. T. Gruber, C. Kirchner, R. Kling, F. Reuss, A. Waag, F. Bertram, D. Forster, J. Christen, and M. Schreck, Appl. Phys. Lett. **83**, 3290 (2003).

17. K. Ellmer, J. Phys. D **33**, R17 (2000).

18. C. Suryanarayana and M.G. Norton, *X-Ray Diffraction: A Practical Approach* (Plenum, New York, 1998).

19. J. Albertsson, S.C. Abrahams, and A. Kvick, Acta Crystallogr. B **45**, 34 (1989).

20. S.H. Park, T. Hanada, D.C. Oh, T. Minegishi, H. Goto, G. Fujimoto, J.S. Park, I.H. Im, J.H. Chang, M.W. Cho, T. Yao, and K. Inaba, Appl. Phys. Lett. **91**, 231 904 (2007).

21. R. Cebulla, R. Wendt, and K. Ellmer, J. Appl. Phys. **83**, 1087 (1998).

22. B. Williamson and R.C. Smallman, Philos. Mag. **1**, 34 (1956).

23. X.S. Wang, Z.C. Wu, J.F. Webb, and Z.G. Liu, Appl. Phys. A **77**, 561 (2003).

24. C.R. Aita and R.J. Lad, J. Appl. Phys. **51**, 6405 (1980).

25. C.R. Aita, A.J. Purdes, R.J. Lad, and P.D. Funkenbusch, J. Appl. Phys. **51**, 5533 (1980).

26. D.J. Ball, J. Appl. Phys. **43**, 3047 (1972).

27. T.E. Mody and J.T. Yates, J. Vac. Sci. Technol. **8**, 525 (1971).

28. I. Brodie, L.T. Lamont, and D.O. Myers, J. Vac. Sci. Technol. **6**, 124 (1969).

29. S. Thomas, J. Appl. Phys. **45**, 161 (1974).

30. J. Verhoeven and J. Las, Surf. Sci. **58**, 566 (1976).

31. Y. Margoninski, D. Segal, and R.E. Kirby, Surf. Sci. **53**, 488 (1975).

32. F. Urbach, Phys. Rev. **92**, 1324 (1953).

33. G.D. Cody, J. Non-Cryst. Solids **141**, 3 (1992).

ОСОБЛИВОСТІ ВПЛИВУ УМОВ ВИРОЩУВАННЯ
НА СТРУКТУРНІ І ОПТИЧНІ ВЛАСТИВОСТІ
ПЛІВОК $Zn_{0,9}Cd_{0,1}O$

І.І. Штеплюк, Г.В. Лашкарьов, В.В. Хомяк, О.С. Литвин, П.Д. Мар'янчук, І.І. Тімофєєва, А.І. Євтушенко, В.Й. Лазоренко

Р е з ю м е

Досліджено вплив потужності магнетрона і співвідношення тисків робочих газів Ar/O_2 на мікроструктуру та оптичні властивості плівок $Zn_{0,9}Cd_{0,1}O$. Плівки осаджено методом магнетронного розпилювання на постійному струмі при температурі підкладки 250 °C. Дослідження морфології поверхні, здійснені за допомогою атомно-силової мікроскопії (АСМ), і рентгенофазовий аналіз (РФА) виявили сильний вплив технологічних параметрів осадження на мікроструктуру плівок. РФА аналіз показав, що всі вирощені плівки є полікристалічними і однофазними. Встановлено, що зростання парціального тиску аргону в газовій суміші $Ar:O_2$ сприятливо впливає на кристалічну структуру твердих розчинів $Zn_{0,9}Cd_{0,1}O$. Обговорено особливості контролю ширини забороненої зони та морфології поверхні твердих розчинів $Zn_{0,9}Cd_{0,1}O$ шляхом зміни параметрів вирощування.